CONF-9509235--1

BNL-62213

ELEMENTARY EXCITATIONS AND PHASE TRANSITIONS IN CRYSTALS

S. M. SHAPIRO, *Brookhaven National Laboratory, Upton, NY 11973 USA*

I. INTRODUCTION

The unique method of measuring elementary excitations in solids over a wide range of energy and momentum transfers is inelastic scattering of neutrons. Elementary excitations are defined as a correlated motion of atoms or spins in a solid which include phonons, magnons, rotons, or crystal field excitations. These excitations play a fundamental role in a wide variety of structural and magnetic phase transitions and provide the information in understanding the underlying microscopic mechanism of the transformation. Below, I shall review some of the relevant aspects of neutron scattering formalism related to inelastic neutron scattering and demonstrate how it has been applied to the study of phase transitions in crystals. I shall give two examples of structural phase transitions where the phonons are the elementary excitations and studies in a conventional superconductor where the phonon linewidths are a measure of the electron-phonon coupling responsible for the pairing.

II. NEUTRON SCATTERING

An inelastic neutron scattering experiment measures the neutron intensity scattered by a sample as a function of momentum ($\mathbf{Q}$) and energy ($\hbar\omega$) transferred to the sample[1]. Energy and momentum conservation governs the scattering process:

$$\mathbf{Q} = \mathbf{k_i} - \mathbf{k_f}$$
$$\hbar\omega = E_i - E_f = \hbar^2/2m_N(k_i^2 - k_f^2) \qquad (1)$$

Where $k_{i(f)}$ and $E_{i(f)}$ are the initial (final) momenta and energy of the neutron and the m_N is the neutron mass..

The observed intensity of the scattered neutrons is proportional to the convolution of the scattering function, $S(\mathbf{Q},\omega)$, and the instrumental resolution function:

$$I(\mathbf{Q}_o,\omega_0) = 1/N\frac{k_f}{k_i}\int S(\mathbf{Q},\omega) \otimes R(\mathbf{Q}-\mathbf{Q}_o,\omega-\omega_0)\, d\omega \qquad (2)$$

For a three axis instrument the four dimensional resolution function, $R(\mathbf{Q},\omega)$ is well known and a very important part of determining the true cross section from the observed intensity[1]. The scattering function contains the information about the positions and motions of the atoms and their spins

and is essentially the Fourier transform of a density-density correlation function:

$$S(Q,\omega) = \int_{-\infty}^{\infty} \langle \rho_Q \rho_{-Q} \rangle e^{-\omega t} dt \qquad (3)$$

where ρ_Q is a density operator which can be either a spin or atomic density. Since most systems studied are in equilibrium, we can employ the fluctuation-dissipation theory which relates the fluctuation properties of a system, which is $S(Q,\omega)$, to the response of the system to an external time-dependent perturbation which is the dynamical susceptibility:

$$S(Q,\omega) = 1/\pi\,(n(\omega) + 1)\,\chi''(Q,\omega) \qquad (4)$$

$(n(\omega) +1) = [1-\exp(-\hbar\omega/kT)]$ is the thermal occupation factor which has the limits $(n(\omega) +1) \sim 1$ for $\hbar\omega >> kT$ and $(n(\omega) +1) \sim n(\omega) \sim kT/\hbar\omega$ for $\hbar\omega << kT$.

Let us now consider separately the case for phonons and magnons. For phonons, the density operator is a time dependent atomic displacement, $u_i(t)$ and the correlation function of Eq. (3) for harmonic phonons is:

$$\langle \rho_Q \rho_{-Q} \rangle \rightarrow \langle \mathbf{Q} \cdot \mathbf{u}_i(0)\, \mathbf{Q} \cdot \mathbf{u}_j(t) \rangle \qquad (5)$$

Using a normal mode expansion for the atomic displacements which is worked out in many textbooks[2], the scattering function becomes.

$$S(\mathbf{Q},\omega) = \frac{(n_j(\omega_j(q)) + 1/2 \pm 1/2)}{\omega_j(q)} \mid F_d(\mathbf{Q}) \mid^2 \delta(E_i - E_f \pm \hbar\omega_j(q))\, \delta(\mathbf{Q} \pm \mathbf{q} - \tau) \qquad (6)$$

where $\mathbf{Q} = \tau + \mathbf{q}$, and τ is a reciprocal lattice vector and $\mathbf{q}$ is the wave vector of the phonon within a Brillouin zone, The inelastic phonon structure factor is:

$$F(Q) = \sum_d \frac{b_d}{\sqrt{M_d}} (\mathbf{Q} \cdot \xi_d(q))\, e^{i\mathbf{Q}\cdot\mathbf{r}}\, e^{-W_d} \qquad (7)$$

where the sum is over d atoms in a unit cell and ξ's are unit vectors in the direction of the atomic displacements about their equilibrium positions for a particular phonon mode. W_d is the Debye-Waller factor.

The frequency $\omega_j(q)$ is determined by the potential seen by each atom which governs many of the properties of the solid such as sound propagation, specific heat, thermal expansion, conductivity, melting and

DISCLAIMER

Portions of this document may be illegible in electronic image products. Images are produced from the best available original document.

superconductivity, if present. Certain vibrational modes, as will be discussed, play a very fundamental role.

For magnetic excitations, the magnetic moment of the neutron couples with the unpaired spins in the solid. For this case the correlation function becomes a spin-spin correlation function:

$$\langle \rho_Q \rho_{-Q} \rangle \rightarrow \langle S_i(0)\, S_j(t) \rangle \tag{8}$$

and the fluctuation dissipation theorem relates the scattering function to the imaginary part of the magnetic dynamical susceptibility. Applying the Kramers-Kronig relationship, the real part of the susceptibility becomes:

$$\chi'(Q) = 1/\pi \int \chi''(Q,\omega)\, d\omega/\omega \tag{9}$$

In the limit $Q \rightarrow 0$, $\chi''(Q)$ is the laboratory measured magnetic susceptibility which is, for the case of non-interacting spins of magnitude S:

$$\chi_o = 1/2(g\mu_B)^2 S(S+1)/kT \tag{10}$$

where g is the Lande g-factor.

The scattering function for magnetic scattering can be written:

$$S(Q,\omega) = (n(\omega) + 1)\, S(S+1)\, \frac{\chi(Q)}{\chi_o}\, \frac{\hbar\omega}{kT}\, F(Q,\omega) \tag{11}$$

The quantity $F(Q,\omega)$ is a normalized spectral shape function and is used to describe the excitation. Usually a Lorentzian centered around $\omega=0$ or $\omega=\omega(q)$ is used to describe critical scattering or scattering from spin waves. The variation of spin waves give a measure of the exchange interactions in the solid. For a Heisenberg ferromagnet with exchange integrals $J_{ii'}$ arising due to electrostatic interactions between the unpaired electrons on atom i and i', the spin wave energy is:

$$\omega(q) = 2S[J(0) - J(q)] \tag{12}$$

with

$$J(q) = \sum_{i'} J_{ii'} \exp(iq\cdot(r_i - r_{i'})) \tag{13}$$

In a ferromagnet, for small q, the dispersion relation is

$$\omega(q) = Dq^2 \tag{14}$$

where $D=2JSa^2$, is the magnetic stiffness with a being the distance between magnetic atoms.

III. PHASE TRANSITIONS

There are many types of phase transitions that occur in nature which include gas-to-liquid, liquid-to-solid, solid-to-solid, superconducting-to-normal, metal-to-insulator, order-to-disorder, and so on. The Landau theory of phase transitions is the universal starting point to describe all these transitions. This phenomenological theory relies on the assumption that the thermodynamic energy can be expanded as a Taylor series about the critical point. The Helmholtz free energy[3] can be written in terms of an order parameter, η:

$$F(T,\eta) = F_0 + 1/2\, a(T)\eta^2 + 1/4\, b\eta^4 + 1/6\, c\eta^6 + \ldots \tag{15}$$

where all the temperature dependence is placed in the coefficient of the quadratic term and has the form

$$a(T) = a_0\,(T-T_c) \tag{16}$$

where T_c is the transition temperature. The order parameter has the

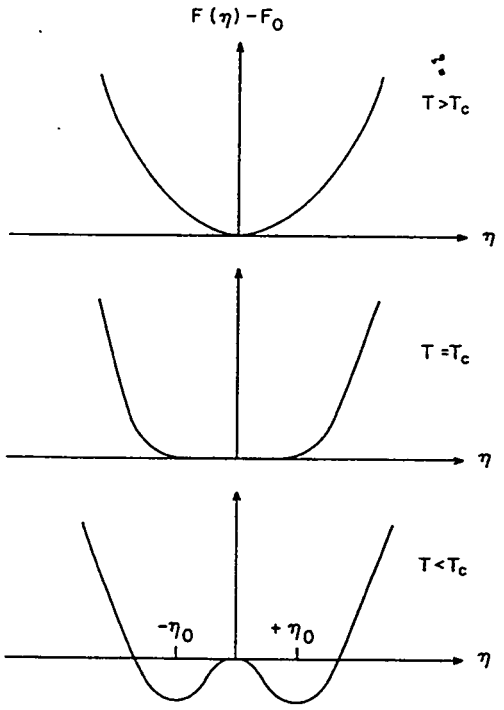

Fig. 1 Plot of free energy function (Eq. (15)) for three different temperatures

properties $\eta = 0$ for $T>T_c$ and $\eta = \eta_0$ for $T<T_c$. In real systems the order parameter could be a magnetization, a spontaneous polarization for a ferroelectric systems, a density for liquid gas systems, or an atomic displacement. The Landau theory does not give the correct answers to many of the measured properties of phase transitions such as the critical exponents, but it does provide excellent insight into the nature of the transition. Figure 1 is a plot of Eq. (15) for various temperatures. For T>Tc, the free energy is parabolic with a minimum at $\eta=0$. For T<Tc the coefficient of the quadratic term is negative so $F(\eta)$ initially decreases with η and then begins to increase as the higher order terms come into play. This gives two minima at $\pm\eta_0$ corresponding to two different domains of the order parameter. For the well known ferromagnetic case, these correspond to a spin-up or a spin-down configuration. In a structural phase transition, η corresponds to an atomic displacement to either side of the high temperature equilibrium position. At $T=T_c$, the free energy is very flat near $\eta=0$ and fluctuations of the order parameter are very large. This is the well known critical fluctuation or opalescence near the transition temperature. The curvature of the free energy, or its second derivative is related to the thermodynamic force and gives the frequency of the fluctuations which varies as:

$$\omega^2 T) \sim (T-Tc) \qquad (17)$$

This critical slowing down is the "soft" mode of the system and the frequency goes to zero as $T \rightarrow Tc$. The soft mode theory of structural phase transitions was proposed by Cochran and Anderson[4] nearly four decades ago and has been ovserved in many structural phase transitions over the years[5]. It states that the displacements associated with a particular lattice vibrational mode are precisely the atomic displacements needed to transform from the higher symmetry to the lower symmetry phase. The low temperature structure looks identical to a snap shot of the atoms participating in the soft mode. The frequency of this mode goes to zero at T_c, since the restoring forces for this mode become zero. The crystal becomes unstable and transforms into the new phase.

Below, I shall give some examples of structural transformations where a particular lattice mode becomes unstable, or nearly so, at the transition temperature.

IV. $SrTiO_3$

The most extensively class of materials studied are those with the perovskite structure with chemical formula: ABX_3. The cell is built up of octahedra of X atoms with B atoms at the center. The soft modes associated with the structural phase transitions occurring in these materials correspond

to rotations of octraheda about axes passing through the vertices of the octahedra.

One of the most investigated systems is SrTiO3 and Fig. 2 gives a summary of the work done over a 25 year period. The top panel (Fig. 2a) shows the inelastic neutron spectrum taken near T_c. The inelastic peak at $\omega=\omega_\infty$ follows the temperature dependence[6] of Eq (17) to within a few degrees of T_c. The narrow peak at $\omega=0$ is the "central peak" whose intensity diverges as T_c is approached[7]. The origin of the central peak is still not clear, but it is sample dependent and appears to be related to defect concentration in the imperfect crystal[8]. Figure 2b shows the result of an x-ray diffraction study[9] of the phase transition in $SrTiO_3$. Because of the much higher energy of x-rays, the energy integral Eq. (6) is measured so no information about the energy scale is obtained. The observed q-scan shows a two component spectrum: a broad feature, reflecting the energy integration over both the phonon and the central peak, and a much narrow part whose presence was unexpected. The half-width of each peak corresponds to an inverse correlation length and this spectrum reveals the problem of the two length scales observed in many magnetic and structural transition by x-ray diffraction measurements. The bottom panel is an attempt to measure the narrow component[10] in a different sample of $SrTiO_3$. Clearly, only the broader peak is present. This is the dilemma posed by recent experiments on structural and magnetic phase transitions: What is the origin of the narrow component? The answer is not fully known but the important observation that the narrow component is readily seen in X-ray experiments and not in a neutron experiment suggests that the narrow component originates in the near surface, or outer skin of the specimen, since the neutron penetrates much more deeply into the sample than an X-ray beam. This was confirmed by a clever neutron experiment on Tb where a spectra similar to Fig. 2b was observed, but at very small scattering angles[11]. In this case the sample was translated through a very narrow beam and the diffracted intensity showed an enhancement of the narrow component in the outer 200 microns of the sample. A neutron experiment of this sort is impossible in $SrTiO_3$, but a synchrotron x-ray experiment was performed using very short wavelength x-rays[12]. This experiment also revealed that when the beam passed through the edge of the crystal, the narrow component was enhanced. We chose another method to characterize the narrow component. A large sample of $SrTiO_3$ was cut into thin slices[10]. Figure 3 shows a high resolution neutron diffraction pattern on a bulk sample of $SrTiO_3$ (top) and a thinly sliced sample (bottom). On the thinly sliced sample the narrow component is observed whereas in the bulk, only the broad component is present. Since the thinly sliced sample has more near surface volume relative to the bulk, the narrow component is visible.

The origin of the narrow component is not fully known, but it has been suggested that strains in the near surface area, which have a relatively long range, couple quadratically to the square of the order parameter[13]. If

this is so, then the transition temperature can be modified and the narrow component reflects that the near surface area has already transformed. These

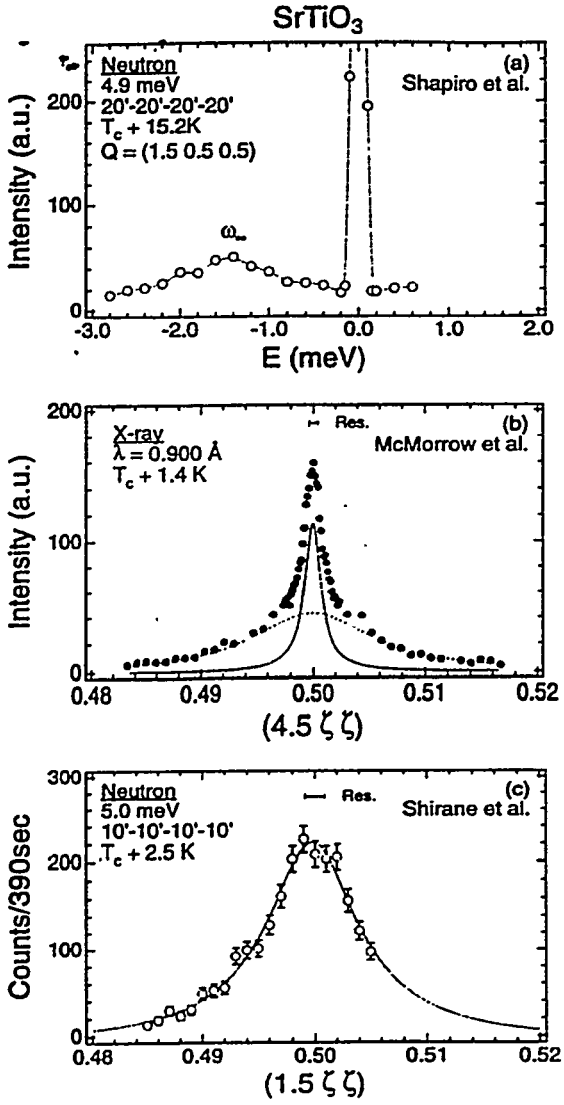

Fig.2 (a) Inelastic neutron-scattering spectrum of SrTiO3 from Ref. 7. clearly showing soft phonon and central peak. (b) X-ray profile measured in Ref. 9 showing two-length scales. (c) High resolution elastic neutron diffraction scan showing only broad component (Ref. 10).

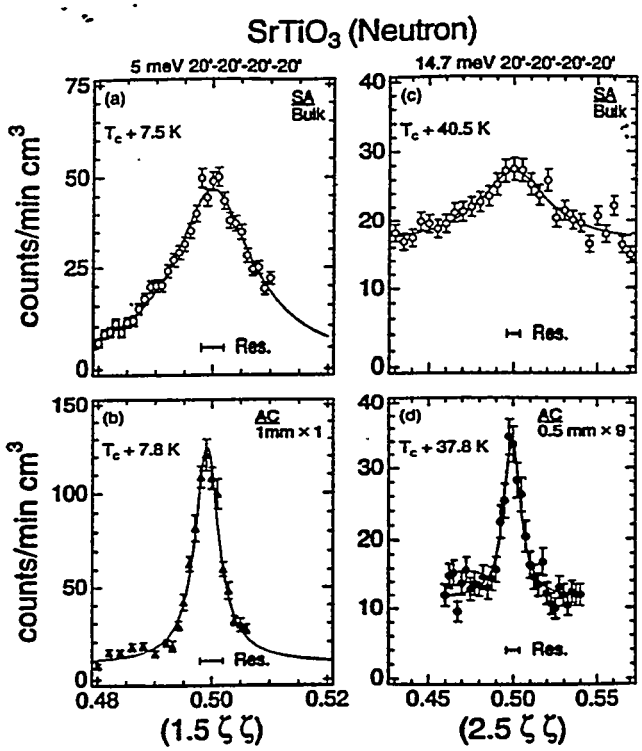

Fig. 3 Neutron diffrtaction peak profiles for SA-Bulk crystal and thin AC crystals taken under indentical spectrometer conditions. Only the narrow component is observed in the thin AC crystal. (Ref. 10)

strains can be extrinsic due to some defects due to the termination of the surface, or may be an intrinsic effect due to different phonon displacements in the near surface region. More theoretical work is needed to explain the feature.

V. MARTENSITIC TRANSFORMATIONS

Martensitic transformations can be defined as first order structural transformations that are displacive, diffusionless where shear strains play a dominant role. Since they are first order, the free energy described in Fig. 1 does not describe the phonon softening in these systems. The Landau free energy of Eq. (14) can be modified by making the fourth order term negative. The potential at $T=T_c$ is not flat as in Fig. 1b, but at T_c there are equal minima at $\eta=0$ and $\eta=\pm\eta_o$ so there is a temperature region where there is a coexistence of the low temperature and high temperature phases. Since the potential wells never become flat, there is not a complete softening of phonon in a first order transition. Nevertheless, there has been extensive neutron studies of systems exhibiting Martensitic transformations which show substantial phonon softening that are precursors to the transformation. Some systems show remarkable softening and others show very little. Below I shall discuss two systems, Ni-Al[14] and Ni_2MnGa[15] that exhibit substantial phonon softening.

The alloy Ni_xAl_{1-x} exhibit Martensitic transformations for $60<x<65$ atomic %. The structure is ordered bcc which is a CsCl-type structure with Ni atoms in the center of a cube and Al atoms on the corners. The excess Ni is distributed randomly over the corner Al sites. Ni_2MnGa is a compound with the fcc Heusler structure. It can be viewed as composed of 8 bcc type cells with Ni atoms at the center and the corners have an ordered arrangement of Mn and Ga. The lattice parameter of Ni_2MnGa (5.822Å) is nearly twice that of Ni_xAl_{1-x} (2.86Å).

The lattice dynamics of these two systems has been studied[14,15]. In both system the $[\zeta\zeta 0]$ transverse acoustic mode has an anomalous low energy and exhibits a very strong temperature dependence. This branch corresponds, in the limit $\zeta\rightarrow 0$ to the elastic constant $C'=1/2(C_{11}-C_{12})$. The atomic displacements of this branch are a sliding of {110} planes along the perpendicular [1-10] direction. Depending upon the repeat distance of the shear, there is a modulation of the cubic lattice. Figure 4 shows the temperature dependence of this branch for the two different systems. Similar behavior exists in that the dispersion curve shows a pronounced softening around the wavevector $\zeta=1/6$ for NiAl and $\zeta=1/3$ for Ni_2MnGa. (These wave vectors are identical if we measure relative to the bcc unit in Ni_2MnGa.) In addition to the dynamical precursors to the phase transition, there is also some elastic diffuse scattering centered at the same wavevector as the phonon anomalies as shown in the lower portions of Fig. 4. Electron diffraction studies of the same two materials shows similar diffuse scattering. This scattering can be imaged and real space pictures of the atomic structure are obtained with atomic scale resolution. Both for Ni_xAl_{1-x} and Ni_2MnGa the cubic system has regions or embryos of low temperature structure imbedded in the cubic matrix. These distortions give rise to the diffuse scattering and the size of these regions are about 1.2 nm which corresponds to the inverse q width of the elastic diffuse scattering.

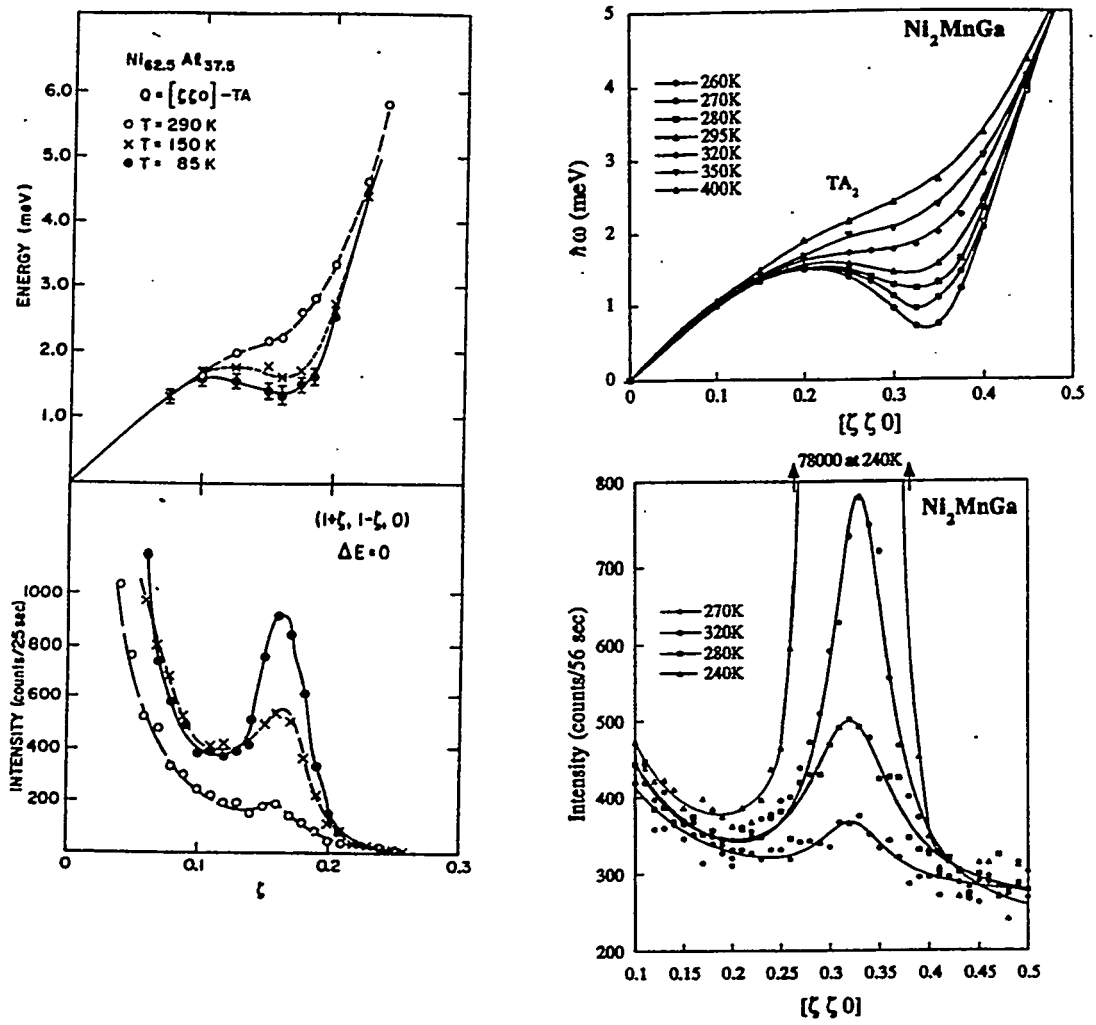

Fig. 4. Left: Ni_xAl_{1-x} (x=62.5): Temperature dependence of the dispersion curve of the [ζζ0] - TA_2 mode and the elastic scattering observed in the [ζζ0] direction (Ref. 14). Right: Ni_2MnGa: Temperature dependece of the anomaly in the [ζζ0]-TA_2 branch and the temperature evolution of the elastic scattering along the same [ζζ0] direction. (Ref 15).

The softening is more pronounced in Ni_2MnGa as shown in Fig. 5 where $\omega^2(T)$ is plotted for the two systems as a function of temperature. They both show a linear temperature dependence. Ni_2MnGa extrapolates to T_0=250K which is slightly higher than the Martensitic transition temperature (T_M=220K). An intermediate phase is predicted from these results to be present in the temperature range $T_1>T>T_M$ where the fcc structure is dynamically unstable. The dramatic increase in the intensity of the elastic

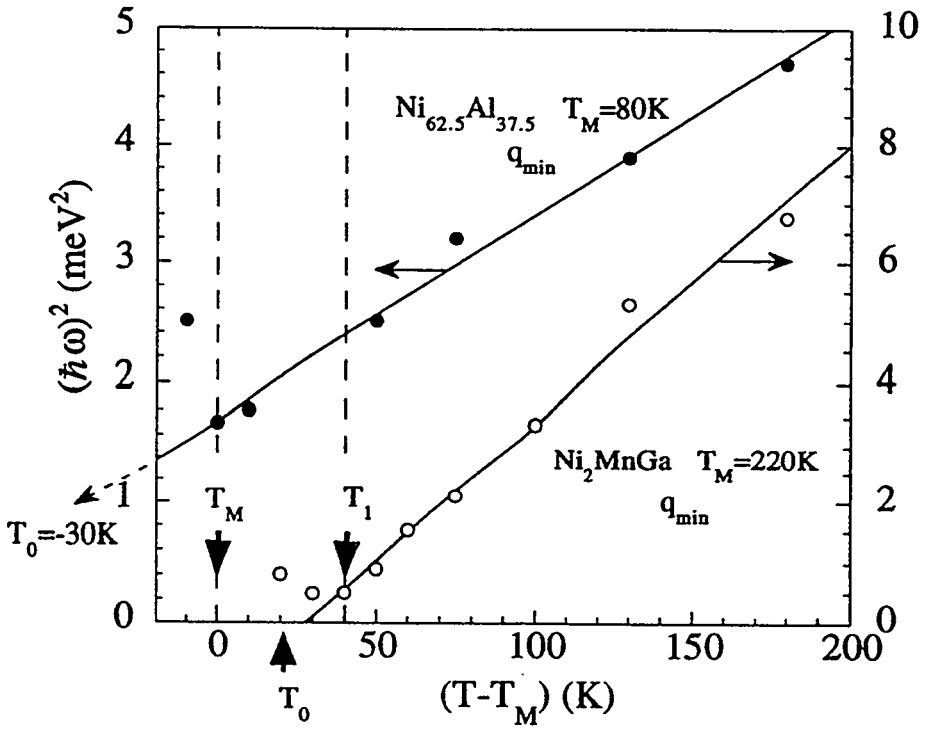

Fig 5. $(\hbar\omega)^2$ vs $T-T_M$ for $Ni_{62.5}Al_{37.5}$ and Ni_2MnGa measured at the soft wavevector q_{min}. The upturn in the soft mode frequence for Ni_2MnGa signals an intermediate phase present between T_1 and T_M, the Martensitic transition temperature

diffuse scattering and the increase of the soft mode frequency below T_1~260 K confirmed this speculation. Below T_1 ~ 260 K the elastic peaks at ζ ~ 0.33 correspond to Bragg scattering in this new phase. This contrasts with known structure of the Martensite phase were there is a five-layer modulation and corresponds to new Bragg peaks at ζ~0.4 which do appear below T_M.

The behavior of the soft mode in Ni-Al extrapolates to a temperature T_o= -40K which is well below T_M=80K. The softening is less complete and the new Bragg peaks that appear at ζ~1/7 are very close to the value ζ~1/6 of the phonon anomaly. There does not appear to be any intermediate or premartensitic phase in Ni-Al although a reinvestigation is warranted.

VI. SUPERCONDUCTIVITY:

I would like to review some older neutron experiments on conventional superconductors which provide a direct measurement of the electron-phonon coupling. These experiments were performed on systems where the mechanism for the superconductivity is understood via the BCS theory and the Cooper pairing is due to the electron phonon (e-p) interaction. The experiments should be looked at again in light of the "new" high T_c compounds where the mechanism for the superconductivity is still being investigated. In addition, the experiments described below exploit several of the subtleties of the triple axis instruments and represent the type of

experiments that will be performed on the intense neutron sources in the future.

Within the BCS theory of superconductivity, the McMillan electron phonon coupling parameter, λ, can be written as[16]:

$$\lambda = \int_0^{\omega_o} \frac{\alpha^2(\omega)F(\omega)}{\omega} d\omega \qquad (18)$$

$\alpha^2(\omega)$ is the average electron-phonon interaction and $F(\omega)$ is the phonon density of states. The integration is over the phonon frequencies. Allen[17] has shown the λ is related to phonon linewidth (2Γ) which is measured in the neutron scattering experiment by:

$$2\Gamma = 2\pi N(0) h\omega^2 \lambda_q \qquad (19)$$

where λ_q is the contribution to λ from the phonon with wave vector q and N(0) is the density of electronic states at the Fermi surface.

The first measurement[18] of the e-p contribution was performed on Nb_3Sn which was, prior to 1987, a high-Tc material with a strong e-p interaction. A subsequent experiment[19] was performed on single crystals of Nb which has T_c=9.2K. Fig. 6 shows the inelastic spectra for a transverse phonon propagating along the [$\zeta\zeta$0] direction for two different temperatures. A change in linewidth is small but easily seen by comparing the peak intensities. Since the thermal population factor ($n(\omega)+1$) should decrease with temperature, the increase in the peak intensities at lower temperature naturally implies a narrowing of the peak. This small change of linewidth was only measurable because there is perfect focusing of the three axis resolution function. This means that the slope of the neutron resolution function is the same as the slope of the dispersion curve for this phonon. Figure 7 shows the temperature dependence of 2Γ for three different phonons with energies relative to the superconducting gap given by the inset in the figure. For the phonons, A and B, the energy at low temperatures is below the gap and the extra linewidth disappears. This is physically understood since this phonon has an energy less than the superconducting gap and does not have enough energy to break up the Cooper pairs. Therefore, this channel of decay is quenched. As the temperature increases to where $h\omega_q = 2\Delta(T)$, the linewidth increases and even reaches a value greater than the normal state. This behavior was predicted[20], via the BCS theory, for the low frequency sound waves measured in an ultrasonic experiment.

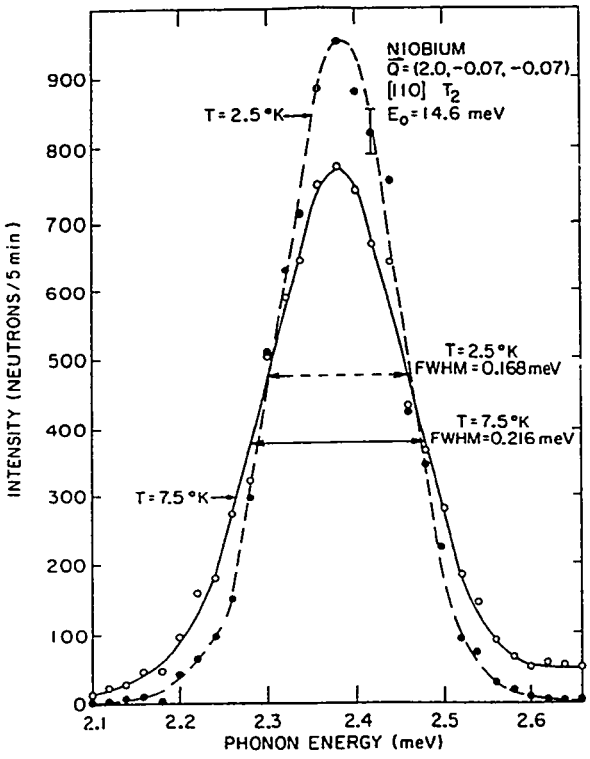

Fig. 6: Neutron group of [ζζ0]TA, ζ=0.07 phonon showing change in line width as the sample becomes superconducting. This corresponds to curve A in Fig. 7 (From ref. 19)

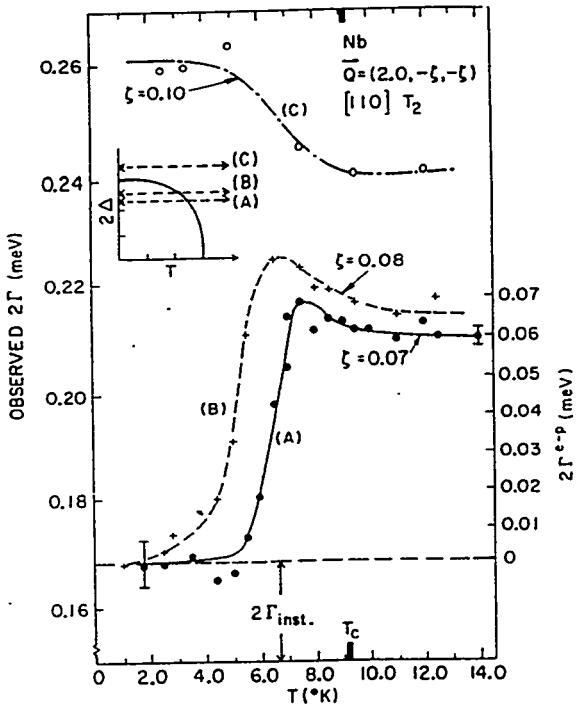

Fig. 7. Temperature dependence of several [ζζ0] TA_2 phonons in Nb showing the change in linewidth due to superconducting gap. Curves A and B have the phonon energy less than the gap energy and curve C the phonon energy is greather than the gap energy. (Ref. 19)

With neutrons, much higher frequency sound is measured and some subtleties of the theory was measurable only in the neutron experiment.

A similar measurement was performed recently on the '214' high-T_c superconductor[21]. No temperature dependence changes of the linewidth were observed near the transition temperature which is consistent with a known low electronic density of states at the Fermi surface, N(0). If one used the calculated value of N(0), λ would have to very large (λ~20) in order to give a measurable energy width. For Nb and other conventional superconductors, λ is typically ~1.0.

VII. CONCLUSIONS

I have presented several cases where inelastic neutron scattering experiments have played a very important role in understanding unusual aspects of different types of phase transitions. It is most likely that this powerful technique will continue to play a dominant role in the future studies, provided that old neutron sources are refurbished and new, more powerful sources will be available in the future.

ACKNOWLEDGMENTS

I thank my many collaborators at Brookhaven and elsewhere who participated in the work described in this paper. The work at Brookhaven is supported by the Division of Materials Science, U.S. Department of Energy under Contract No. DE-AC02-76CH00016. Part of this work was carried out as part of the U. S. - Japan Cooperative Neutron Scattering Program.

REFERENCES

1. There are many excellent textbooks related to Neutron Scattering. Of particular value are: G. E. Bacon, *Neutron Diffraction* (Clarendon Press, Oxford, 1975); *S. W. Lovesey*, Theory of Neutron Diffraction (Oxford University Press, London 1984); G. L Squires, *Introduction to the Theory of Thermal Neutron Scattering* (Cambridge Press, New York 1978)

2. M. J. Cooper and R. Nathans, Acta Cryst. **23**, 357 (1967), M. Nielsen and H. B. Møller, Acta Cryst. **A25**, 547 (1969), N. J. Chesser and J. D. Axe, Acta Cryst. **A29**, 160 (1973)

3. H. E. Stanely, *Introduction to Phae Transitions and Critical Phenomena* (Oxford, New York, 1971)

4. W. Cochran, Adv. Phys. **9**, 387 (1961); P. W. Anderson, Fizika Dieleckrikov, G. F. Skanavi, Ed., Acad. USSR, Moscow, p. 290 (1960)

5. G. Shirane, Rev. of Mod, Phys., **46**, 437 (1974)

6. G. Shirane and Y. Yamada, Phys. Rev. **177**, 858 (1969)

7. S. M. Shapiro, J. D. Axe, G. Shirane, and T. Riste, Phys. Rev. **B6**, 4332 (1972)

8. J. B. Hastings, S. M. Shapiro, and B. C. Frazer, Phys Rev. Lett. **40**, 237 (1978)

9. D. F. McMorrow, N. Hamaya, S. Shimonmua, Y. Fujii, S. Kishimoto, and H. Iwasaki, Solid State. Commun. **76**, 443 (1990)

10. G. Shirane, R. A. Cowley, M. Matsuda, and S. M. Shapiro, Phys. Rev. **B48**, 15595 (1993); K. Hirota, J. P. Hill, S. M. Shapiro, G. Shirane, and Y. Fujii, Phys. Rev. (in press)

11. P. M. Gehring, K. Hirota, C. F. Majkrzak, and G. Shirane, Phys. Rev. Lett. **71**, 1087 (1993)

12. H. B. Neumann, U. Rütt, J. R. Schneider, and G. Shirane, Phys. Rev. (in press).

13. J. D. Axe and R. A. Cowley (private communication)

14. S. M. Shapiro, B. X. Yang, Y. Noda, L. E. Tanner and D. Schryvers, Phys. Rev. **B44**, 9301, (1991)

15. A. Zheludev, S. M. Shapiro, P. Wochner, A. Schwartz, M. Wall, and L. E. Tanner, Phys. Rev., **B51**,11310, (1995)

16. W. L. McMillan, Phys. Rev. **167**, 331 (1968)

17. P. B. Allen, Phys. Rev. **B6**, 2577 (1972); Solid State Commun. **14**, 937 (1974)

18. J. D. Axe and G. Shirane, Phys. Rev. Lett. **30**, 214 (1973); Phys. Rev. **B8**, 1965 (1973).

19. S. M. Shapiro, G. Shirane, and J. D. Axe, Phys. Rev. **B12**, 4899 (1975)

20. V. M. Bobetic, Phys. Rev. **136**, A1535 (1964)

21. H. Chou, K. Yamada, J. D. Axe, S. M. Shapiro, G. Shirane, I. Tanaka, K. Yamane, and H. Kojima, Phys. Rev. **B42**, 4273 (1990).